Applicability of the deformation-potential approximation to deep donors in silicon

K. Bergman, G. Grossmann, and H. G. Grimmeiss
Department of Solid State Physics, University of Lund, Box 118, S-221 00 Lund, Sweden

Michael Stavola
AT&T Bell Laboratories, Murray Hill, New Jersey 07974-2070

Robert E. McMurray, Jr.
Lawrence Berkeley Laboratory, University of California, Berkeley, California 94720
(Received 26 July 1988)

Several deep double donors due to sulfur and selenium impurities, both isolated and in pairs, have been investigated in infrared-absorption and uniaxial-stress experiments. The study of several similar centers in their different charge states allows trends in parameters to be revealed. Particular attention is given to the applicability of effective-mass theory (EMT) and the deformation-potential approximation (DPA) to the various states studied. The *np* excited states are well described by EMT and hence their behavior under stress by the DPA. The deep 1*s* ground states do not follow DPA but shift linearly with respect to the center of gravity of the conduction bands with shift rates that increase with the ionization energy of the centers. Excited 1*s* states which are deeper than predicted by EMT are also observed to deviate from DPA. A perturbation approach beyond the DPA is developed to fit and compare data. For nontetrahedral centers the stress lifts their orientational degeneracy. The $1s(A_1^+)\rightarrow ns$ transitions of chalcogen pairs are well described by DPA if matrix elements that couple the *ns* states are accounted for. For some centers, stress-induced crossings between allowed and forbidden states reveal information on states [$1s(E)$ and spin-triplet states] that are not accessible by dipole transitions.

I. INTRODUCTION

Sulfur and selenium give rise to a number of different deep donor centers in silicon.[1,2] Several of these defects have been studied in detail using high-resolution Fourier-transform spectroscopy.[2] From these measurements it is known that chalogens such as sulfur and selenium show very pronounced Rydberg series of excited states. As in the case of shallow group-V single donors,[3] these are well described by effective-mass theory (EMT). In contrast to the shallow donors, dipole transitions from the deep ground state to valley-orbit-split *ns* states are—when allowed by symmetry—rather strong at the chalcogen centers, because the ground state can no longer be described within EMT. The valley-orbit splitting, which is most pronounced for 1*s* states, reflects the local symmetry of the center and the observed dipole selection rules governing the transitions between the valley-orbit-split *s* states give information on the defect symmetry.

In this study we examine how well EMT and the deformation-potential approximation (DPA) describe the behavior under stress of the rich electronic structure associated with several sulfur and selenium related centers. The deep 1*s* ground states, the valley-orbit-split 1*s* excited states, and the Rydberg series of excited states are studied for the neutral and singly ionized charge states of isolated impurities and impurity pairs with the exception of the charged Se pairs. A perturbation approach beyond DPA is used to fit our data when required. The parameters that characterize the behavior of the various centers and charge states under stress are compared to reveal trends.

The centers are labeled following the notation by Janzén *et al.*,[2] where the superscript of the label is the charge state of the center before excitation while a subscript 2 indicates a center consisting of a pair of atoms. For example, D^0 and D_2^+ denote the neutral charge state of an isolated center and the ionized charge state of a pair, respectively. To facilitate comparison with other studies, the ground-state binding energies of the different centers are given in Table I together with their respective labels.

One might expect double donors with two bound electrons to bear a greater resemblance to helium than to hydrogen. However, all observed transitions for the neutral charge state correspond to one-electron excitations from the doubly occupied $1s(A_1)$ ground state which leave one of the two electrons in a ground-state orbital. This inner electron is highly localized compared with the extended orbital of the excited electron, as witnessed by ESR and electron-nuclear double resonance (ENDOR).[4,5] Thus, as far as all one-electron excitations are concerned, the inner electron shields the double charge of the core effectively, letting the outer electron experience a closely hydrogenlike potential.[6] However, many-electron effects are clearly observed and may be substantial when the outer electron can penetrate the core, as is the case in the $1s(A_1)1s(T_2)$ configuration,[7] for which the spin-triplet states have been identified in uniaxial-stress[8] studies. Spin-triplet states will only be discussed briefly here be-

TABLE I. Binding energies and corresponding labels of the seven centers studied.

Center	Binding energy (meV)	(Binding energy) (cm^{-1})
S_2^0	187.61[a]	(1513.2)
Se_2^0	206.44[a]	(1665.0)
Se^0	306.63[a]	(2473.1)
S^0	318.32[a]	(2567.4)
S_2^+	371.1[a]	(2993)
Se^+	593.3[b]	(4785)
S^+	613.5[b]	(4948)

[a]Reference 2.
[b]Reference 32.

cause they have been described in detail elsewhere.[8,9]

The binding energies of $1s(E)$ states to which dipole transitions are forbidden have earlier been inferred from Fano resonance experiments.[10] We show here how uniaxial-stress experiments may confirm these assignments.

Recently, Krag *et al.* have published a reevaluation of their results on sulfur-related centers.[11,12] Our analysis of the spectra and the stress dependences differ in some instances from that of Krag *et al.*; new aspects of the sulfur centers are revealed at the highest stresses attained in the present study.

II. SAMPLE PREPARATION AND EXPERIMENTAL METHODS

The samples for this study were prepared by diffusion in sealed quartz ampoules at 1200 °C between 60 h and 3 weeks. The amount of dopant in the ampoules was estimated to give a vapor pressure of about 1 atm at the process temperature. The quenching procedure after diffusion affects the concentration ratios between different types of centers. The samples were quenched in air to produce isolated centers. If pairs were desired, the samples were left in the furnace, which was switched off and allowed to cool to approximately 500 °C over approximately 2 h before the samples were removed. Both Czochralski and float-zone Si crystals were used, with resistivities ranging from 6 to 1000 Ω cm for n-type samples and from 2 to 14 Ω cm for p-type samples. n-type samples were used for the study of neutral centers, and p-type material to obtain charged centers, where different resistivities were used to adjust the Fermi level. Before diffusion, the samples were lapped, polished, and etched to remove sawing damage. Since the chalcogen dopants tend to attack the surface of the samples at elevated temperature, the samples were gently repolished after diffusion. After orientation of the crystal axes by x-ray Laue backscattering, samples were cut to typically $2\times2\times6$ mm^3. The sample dimensions were measured using a micrometer. The spectra were recorded using a Bomem DA3.02 Fourier-transform infrared (FTIR) spectrometer equipped with cooled InSb and $Hg_{1-x}Cd_xTe$ detectors. A continuous-flow He cryostat was used to provide sample temperatures around 10 K. After lapping the end surfaces parallel, the samples were mounted in a stress apparatus where stress is applied to the sample by a pneumatic cylinder via a push-rod. The force is calculated from the gas pressure in the cylinder, which is monitored on a precision gauge. A wire grid polarizer on a KRS-5 substrate was used to study the polarization selection rules.

Typical spectra are presented in Fig. 1, showing that the spectral lines remain sharp up to the highest stresses. A convenient measure of the inhomogeneity of the stress field in the sample is the ratio of the stress-induced broadening to the line shift. In our experiments this ratio was on the order of 5%.

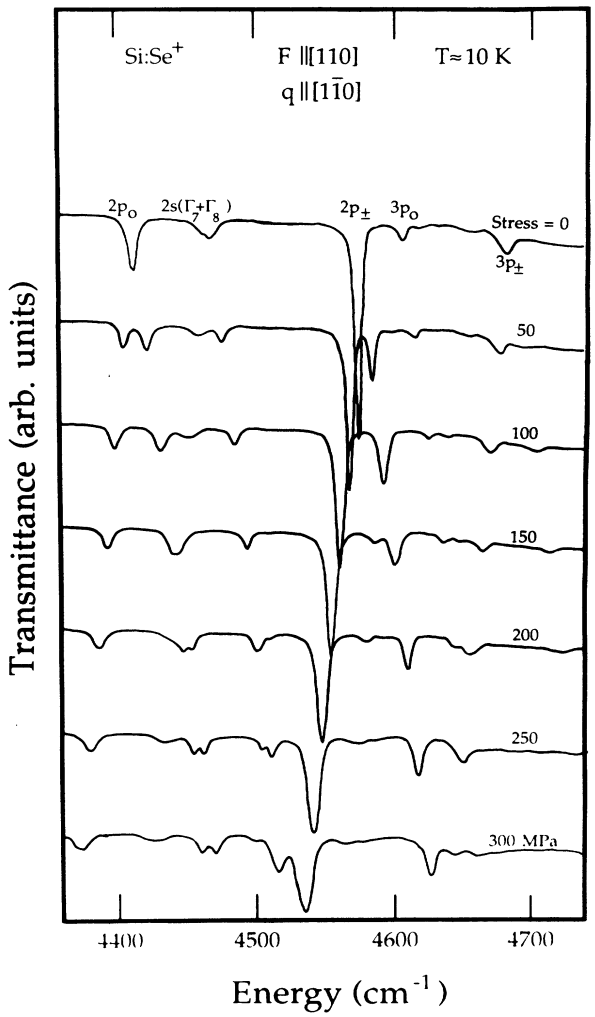

FIG. 1. Spectra of transitions to the higher excited states of $Si:Se^+$ taken for a series of [110] stresses using unpolarized light along [1$\bar{1}$0]. The spectral lines have been labeled according to their final states and remain sharp even when their stress-induced splittings become as large as 100 cm^{-1}.

III. THEORETICAL CONSIDERATIONS

A. Effective-mass theory

The extended excited orbitals of the chalcogen donors in silicon are well described by EMT.[13,2] The s states are split by central cell effects and valley-orbit interaction, and their wave functions are written as symmetry-adapted linear combinations:

$$\Psi = \sum_{j=1}^{6} \alpha_j F_j(\mathbf{r})\phi_j(\mathbf{r}) , \tag{1}$$

where the sum is taken over the six $\langle 100 \rangle$ conduction-band minima. The $F_j(\mathbf{r})$ are hydrogenic EMT envelope functions, and the $\phi_j(\mathbf{r})$ are Bloch functions from the bottom of each valley. For centers with T_d symmetry (such as the isolated substitutional[14,15] chalcogen centers) the six ns states split into an $ns(A_1)$, an $ns(T_2)$, and an $ns(E)$ state.[16] The coefficients α_j of the different linear combinations are given by

valley:			$\hat{\mathbf{x}}$	$-\hat{\mathbf{x}}$	$\hat{\mathbf{y}}$	$-\hat{\mathbf{y}}$	$\hat{\mathbf{z}}$	$-\hat{\mathbf{z}}$
A_1	a_1	$\frac{1}{\sqrt{6}}$	(1	1	1	1	1	1)
E	θ	$\frac{1}{\sqrt{12}}$	(−1	−1	−1	−1	2	2)
	ε	$\frac{1}{2}$	(1	1	−1	−1	0	0)
T_2	x	$\frac{1}{\sqrt{2}}$	(1	−1	0	0	0	0)
	y	$\frac{1}{\sqrt{2}}$	(0	0	1	−1	0	0)
	z	$\frac{1}{\sqrt{2}}$	(0	0	0	0	1	−1)

(2)

The $1s(A_1)$ orbital is the only $1s$ orbital with nonvanishing amplitude at the impurity, thus an electron in this orbital will be affected more by the central cell potential than if it were in the $1s(E)$ or $1s(T_2)$ orbitals. If the central cell potential is attractive, the $1s(A_1)$ state is the ground state, as it is for all isolated centers in this study. The binding energy of the $1s$ state in one-valley EMT is 31.26 meV. Scaling atomic values, one can estimate the ionization energy of the $1s(A_1)^2$ ground state of a He-like double donor D^0 to be about 56 meV, while for D^+ one obtains 125 meV by multiplying the EMT value by 4 to account for the double charge of the core. As can be seen from Table I, the effect of the central cell potential is formidable not only for D^0, but also for D^+. The $1s(T_2)$ and $1s(E)$ states of the neutral centers, however, remain within a few meV from the 31.26-meV value. The corresponding states of the D^+ centers are somewhat deeper than 125 meV. Altarelli[17] has shown that this effect is partly explained by a greater valley-orbit interaction at these ionized centers. As discussed below, the behavior of the $1s(T_2)$ states of D^+ under uniaxial stress also indicates that these states are too deep for EMT to be valid.

In T_d symmetry electric dipole transitions will be symmetry allowed from the $1s(A_1)$ ground state to the $1s(T_2)$ excited state,[7] but not to the $1s(E)$ state. If the $1s(A_1)$ envelope function were hydrogenic as given by EMT, the transition probability from the ground state to the $1s(T_2)$ state would be close to zero as is the case for the shallow group-V donors. For these donors the ionization energies and thus envelope functions are close to EMT. For the deepest group-V donor, Bi, with an ionization energy of 70.98 meV,[18] weak transitions to the $1s(T_2)$ state have been observed,[19] demonstrating that the ground-state envelope function already deviates significantly from EMT for this binding energy. For the chalcogen donors studied here, the ionization energies are much larger and the oscillator strengths of the $1s(A_1) \rightarrow 1s(T_2)$ transitions are comparable to those of the $1s(A_1) \rightarrow 2p_0$ or $1s(A_1) \rightarrow 2p_\pm$ transitions. The deeper the donor, the stronger the relative strength of the $1s(A_1) \rightarrow 1s(T_2)$ transition.

The $D_2{}^0$ and $D_2{}^+$ centers are trigonal centers oriented along the $\langle 111 \rangle$ axes, and from optical experiments[2] their point group has been determined to be D_{3d}. The symmetry-adapted linear combinations of single-valley s states for a center oriented along [111] are given below:

valley:			$\hat{\mathbf{x}}$	$-\hat{\mathbf{x}}$	$\hat{\mathbf{y}}$	$-\hat{\mathbf{y}}$	$\hat{\mathbf{z}}$	$-\hat{\mathbf{z}}$
A_1^+	a_1^+	$\frac{1}{\sqrt{6}}$	(1	1	1	1	1	1)
E^+	θ^+	$\frac{1}{\sqrt{12}}$	(−1	−1	−1	−1	2	2)
	ε^+	$\frac{1}{2}$	(1	1	−1	−1	0	0)
A_1^-	a_1^-	$\frac{1}{\sqrt{6}}$	(1	−1	1	−1	1	−1)
E^-	θ^-	$\frac{1}{\sqrt{12}}$	(−1	1	−1	1	2	−2)
	ε^-	$\frac{1}{2}$	(1	−1	−1	1	0	0)

(3)

Since D_{3d} point group is the direct product of C_{3v} and i (inversion), we have chosen the irreducible representations of the C_{3v} point group as labels; parity is indicated by a plus sign for even and minus sign for odd parity. The $1s(A_1^+)$ state is believed to be the ground state.[20] The components of the electric dipole operator transform as A_1^- and E^-, and hence transitions to $1s(E^+)$ are forbidden by parity. This is consistent with experiment, since only two absorption lines due to $1s(A_1^+) \rightarrow 1s$ transitions are visible in absorption for the $D_2{}^0$ and $D_2{}^+$ centers. If the point group were C_{3v} instead of D_{3d}, parity would not be a good quantum number and we would expect three spectral lines, which in fact have been observed by Wagner *et al.*[21] for mixed pairs of S and Se. The energies of the $1s(E^+)$ states for both S and Se neutral pairs, on the other hand, have been deduced from phonon-assisted Fano resonances,[10] thus all valley-orbit split $1s$ states are accounted for.

B. The deformation-potential approximation

The behavior of electron states of donors in silicon under uniaxial stress is often well described by the deformation-potential approximation.[22,23,3] This is certainly the case if the states in question are well approximated by one-valley EMT, i.e., for all non-s states, which will follow their respective band edges rigidly. Further, states which are well described by Eq. (1), i.e., which are linear combinations of contributions from narrow regions around each band minimum, also follow DPA under stress. Their envelope functions may differ from EMT but will be sufficiently extended in real space for the Fourier transform to remain confined to small regions of $\mathbf{k}$ space. States which do not fulfill these conditions require an analysis extended beyond DPA, which will be discussed in Sec. III C.

Uniaxial stress applied to a multivalley semiconductor crystal will cause shifts in the energies of the conduction-band minima. For a semiconductor with $\langle 100 \rangle$ conduction-band minima like silicon, the shift of the jth minimum with respect to the center of gravity of the conduction bands is given by

$$\delta E^{(j)} = \Xi_u (s_{11} - s_{12}) [(\bar{n} \cdot \bar{j})^2 - \tfrac{1}{3}] T \ . \tag{4}$$

Here Ξ_u is the shear deformation potential, s_{11} and s_{12} are components of the elastic compliance tensor, $\bar{n}$ is a unit vector in the direction of the force, and T is the magnitude of the applied stress (negative for compression). The shift of the valleys with respect to the center of gravity is given in Table II for stress directions of high symmetry.

As already mentioned, non-s states will follow their respective conduction-band valley, and their splitting pattern with respect to shift rates, relative intensities of transition lines, and polarization selection rules can therefore be deduced from the information given in Table II and from the symmetries of the envelope functions. The polarization selection rules of $1s(A_1) \rightarrow np$ transitions are given in Figs. 2(a) and 2(b) for stresses along [001] and [110]; the rules for [111] stress are trivial since the lines do not split.

Since s states contain contributions from different valleys, their behavior under uniaxial stress is more complicated, but may be determined using perturbation theory.

TABLE II. Stress-induced shifts of the conduction-band valleys with respect to the center of gravity according to the deformation-potential approximation (DPA).

Stress direction	Valleys	Shift in energy with respect to center of gravity
$\mathbf{F}\|\|[001]$	$\hat{x}, -\hat{x}, \hat{y}, -\hat{y}$	$-\Delta$
	$\hat{z}, -\hat{z}$	2Δ
$\mathbf{F}\|\|[110]$	$\hat{z}, -\hat{z}$	$-\Delta$
	$\hat{x}, -\hat{x}, \hat{y}, -\hat{y}$	$\frac{\Delta}{2}$
$\mathbf{F}\|\|[111]$ all minima		0
$\Delta = \Xi_u (s_{11} - s_{12}) T/3$		

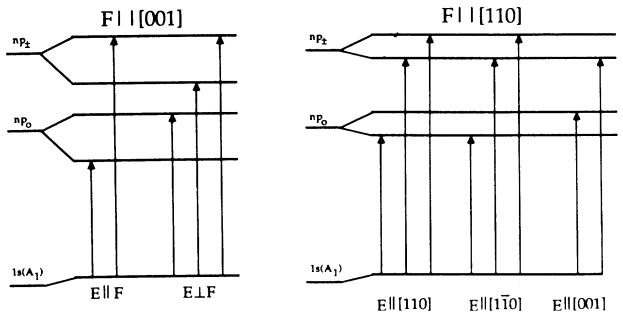

FIG. 2. Polarization selection rules for $1s \rightarrow np$ transitions with uniaxial stress applied along [001] and [110].

Assuming that these states can be decomposed into contributions from each valley which under uniaxial stress follow their respective band edge, matrix elements between s states of the strain perturbation V are given by (disregarding the center-of-gravity shift)

$$\langle \Psi_k | V | \Psi_l \rangle = \sum_{j=1}^{6} \alpha_j^{(k)} \alpha_j^{(l)} \delta E^{(j)} \ . \tag{5}$$

These matrix elements, evaluated within a manifold of degenerate states [e.g., $1s(T_2)$ or $1s(E)$ in T_d symmetry], determine the splitting pattern. In Table III the expectation values of the perturbation are given for the $1s(A_1)$, $1s(T_2)$, and $1s(E)$ states according to Eq. (5). Using Eq. (5) to obtain matrix elements coupling different states, e.g., $1s(A_1)$ and $1s(E)$ in T_d, one must further assume the envelope functions to be equal. If their overlap is less than one, the coupling matrix elements will be reduced and the shear deformation potential Ξ_u obtained from a fit to the coupling observed in experiment will be smaller than that obtained from the splitting of non-s states.[24,18] Evaluating the matrix elements for forces $\mathbf{F}$ applied along the high symmetry directions used in our experiments ($\mathbf{F}\|[001]$, [110], and [111]), it becomes clear that only the states labeled a_1 and θ are mixed by the stress; for the trigonal centers only equal-parity a_1 and θ states mix.

The mixing of the $1s(A_1)$ ground state and the $1s(E)$ excited states under stress is clearly visible for shallow donors,[24,18] although the effect is smaller than calculated using the conduction band Ξ_u. The disagreement between theory and experiment increases with the binding energy of the donor, which confirms that the deviation of the ground-state envelope function from simple EMT reduces the coupling. For the isolated chalcogen centers studied in this work we do not observe any coupling, which is not surprising, since the ground state and the $1s(E)$ state lie more than 150 meV apart even for the most shallow centers. However, the effect on A_1^- and E^- states of $D_2{}^0$ and $D_2{}^+$ centers is quite pronounced, as will be seen below.

C. Uniaxial-stress effects beyond DPA

To the same extent as the ground state deviates from the EMT description, DPA fails to describe its behavior under stress. This is also the case for certain excited

TABLE III. Stress dependence of the valley-orbit-split $1s$ states of a donor in T_d symmetry according to the deformation-potential approximation (DPA). Coupling between the a_1 and θ states has been neglected.

T_d irreducible representation	Electron state	Shift in energy F‖[001]	F‖[110]	F‖[111]
A_1	a_1	0	0	0
T_2	x	$-\Delta$	$+\Delta/2$	0
	y	$-\Delta$	$+\Delta/2$	0
	z	$+2\Delta$	$-\Delta$	0
E	θ	$+\Delta$	$-\Delta/2$	0
	ε	$-\Delta$	$+\Delta/2$	0

$\Delta=\Xi_u(s_{11}-s_{12})T/3$

states with large binding energies. Moreover, the D_2 centers consist of pairs of atoms along the four different $\langle 111\rangle$ axes of the silicon lattice. At zero stress, these centers are orientationally degenerate, but uniaxial stress may lift this degeneracy.

To linear order in the strain ε, we write the perturbation in Cartesian coordinates as

$$V=\sum_{i,j=1}^{3} V_{ij}\varepsilon_{ij} , \tag{6}$$

where the $\{V_{ij}\}$ are electronic operators. The DPA is obtained by applying this perturbation to band states. From the symmetry of the conduction bands at the minima along the $\langle 100\rangle$ directions in silicon, it follows that the linear shifts of the valleys can be expressed in terms of two independent deformation potential constants, Ξ_u (dilation) and Ξ_d (shear).[23] In this section we apply the perturbation V to arbitrary defect states to obtain the splitting pattern and the interaction between states. The DPA results given above are recovered as the limiting case for extended EMT-like states. In this limit the parameters of the general case either vanish or become expressible in terms of Ξ_u and Ξ_d.

To exploit the symmetry of the defect, we write Eq. (6) in irreducible tensor form

$$V=\sum_{\Gamma,r} V_{\Gamma,r}\varepsilon_{\Gamma,r} , \tag{7}$$

where the r's are the row indices of the irreducible representations Γ of the appropriate point group. The only operators that to first order can shift the nondegenerate ground state or the center of gravity of degenerate excited states are those that are invariant under the point group, i.e., belong to A_1, whereas noninvariant operators may lift electronic degeneracies.

In T_d symmetry, the second-rank symmetric tensor ε decomposes into the irreducible representations A_1, E, and T_2, and thus we have

$$V=V_{A_1}\varepsilon_{A_1}+V_{E,\theta}\varepsilon_{E,\theta}+V_{E,\varepsilon}\varepsilon_{E,\varepsilon} +2(V_{T_2,x}\varepsilon_{T_2,x}+V_{T_2,y}\varepsilon_{T_2,y}+V_{T_2,z}\varepsilon_{T_2,z}) , \tag{8}$$

with

$$V_{A_1}=\frac{1}{\sqrt{3}}(V_{xx}+V_{yy}+V_{zz}) ,$$

$$V_{E,\theta}=\frac{1}{\sqrt{6}}(2V_{zz}-V_{xx}-V_{yy}) ,$$

$$V_{E,\varepsilon}=\frac{1}{\sqrt{2}}(V_{xx}-V_{yy}) ,$$

$$V_{T_2,x}=V_{yz},\quad V_{T_2,y}=V_{zx} ,$$

and

$$V_{T_2,z}=V_{xy} ,$$

and where the $\varepsilon_{\Gamma,r}$ are defined analogously.

Changes in the transition energies observed in experiment are due to the difference in shift rate of the final and initial states. These shift rates are determined by the invariant operators V_{A_1}, which for degenerate excited states only affect their center of gravity. We define the transition stress parameter $\mathcal{A}_1$ as

$$\mathcal{A}_1=\frac{1}{\sqrt{3}}(\langle e|V_{A_1}|e\rangle-\langle g|V_{A_1}|g\rangle) , \tag{9}$$

where e stands for excited state and g for ground state. In a one-electron picture, e.g., for a single donor, $\mathcal{A}_1$ measures the difference in shift rate between the excited and the ground state of the electron. If one assumes that the EMT-like excited states follow the conduction bands rigidly, $\mathcal{A}_1$ obtained from $1s(A_1)\rightarrow np$ transitions determines the shift in energy of the ground state relative to the center of gravity of the conduction bands, which is given by $\mathcal{A}_1(s_{11}+2s_{12})T$. For shallow donors where also the ground state is described by EMT, $\mathcal{A}_1$ will be zero. For a double donor with two interacting electrons, the one-electron picture breaks down and $\mathcal{A}_1$ can no longer be related to the stress behavior of one-particle levels.

Perturbation operators of E and T_2 symmetry lead to the splitting of degenerate excited states, i.e., of the $1s(T_2)$ and $1s(E)$ states in T_d symmetry. We consider operators of E symmetry first. To obtain the splitting patterns we have to evaluate the matrix elements within the degenerate set of states, i.e., within the bases of the irreducible representations E and T_2. Since the reductions

of the direct products $E\times E=A_1+A_2+E$ and $T_2\times T_2=A_1+E+T_1+T_2$ both contain E once, nonvanishing matrix elements are allowed by symmetry. Furthermore, all matrix elements within each degenerate set can be expressed in terms of one parameter: given one matrix element all others are simply related to it by the Wigner-Eckart theorem using coupling coefficients given by, e.g., Griffith.[25] The matrix elments between E states can all be expressed in terms of the parameter

$$\mathcal{B}=\frac{1}{\sqrt{6}}\langle E,\theta|V_{E,\varepsilon}|E,\varepsilon\rangle \ . \tag{10}$$

The corresponding secular matrix is given by Kaplyanskii,[26] merely replacing the tensor elements of σ by those of ε. In Ref. 26 the perturbation is defined as a function of stress instead of strain which introduces compliance tensor elements into our expressions for the shifts. As long as the $1s(E)$ states are well described by EMT, DPA yields $\mathcal{B}=-\Xi_u/6$. The resulting splitting pattern is given in Table III. For T_2 states we similarly define the parameter $\mathcal{B}'$ as

$$\mathcal{B}'=\frac{\sqrt{2}}{3}\langle T_2,x|V_{E,\varepsilon}|T_2,x\rangle \ , \tag{11}$$

which reduces to $\Xi_u/3$ within EMT and DPA. From the secular matrix[26] one obtains the splitting pattern of $1s(T_2)$ states given in Table III. For the $1s(T_2)$ states of D^+ centers, which have the largest binding energies of all excited states of the chalcogen donors (considerably larger than expected from EMT), we find significant deviations of $\mathcal{B}'$ from its DPA value $\Xi_u/3$. Operators of E symmetry thus yield splitting patterns for E and T_2 states which are similar to those of the DPA but the parameters will in general differ from the DPA values.

All matrix elements of operators of T_2 symmetry vanish in DPA. For the deep $1s(T_2)$ states of D^+, however, V_{T_2} introduces an observable coupling with matrix elements determined by the parameter

$$\mathcal{C}=2\langle T_2,y|V_{T_2,x}|T_2,z\rangle \tag{12}$$

and the secular matrix again given in Ref. 26.

Noninvariant operators not only cause a splitting of excited states but may also lead to a coupling of excited states. Operators of E symmetry may couple the $1s(A_1)$ to the $1s(E,\theta)$ state. As mentioned in Sec. III B above, for EMT-like ground states the coupling strength is simply related to Ξ_u. Finally, since $E\times T_2=T_1+T_2$, V_{T_2} may also contribute to the interaction between $1s(E)$ and $1s(T_2)$ states, which is observed when these states are shifted into resonance by the uniaxial stress.

Centers with D_{3d} symmetry may be oriented along any of the $\langle 111\rangle$ axes of the cubic lattice. At zero stress, the electronic states of these centers are energetically degenerate, but uniaxial stress applied to the crystal may lift this orientational degeneracy. Studying the effect of stress applied along a given axis on inequivalent centers is equivalent to studying the effect of inequivalent stress directions on one center with a definite orientation, i.e., [111]. For C_{3v} or D_{3d} symmetry, V contains two contributions from operators transforming as A_1: $V_{A_1}\varepsilon_{A_1}$ and $V_{A_1'}\varepsilon_{A_1'}$, where

$$V_{A_1}=\frac{1}{\sqrt{3}}(V_{xx}+V_{yy}+V_{zz})$$

and

$$V_{A_1'}=\frac{1}{\sqrt{3}}(V_{yz}+V_{zx}+V_{xy}) \ .$$

The $\varepsilon_{\Gamma,r}$ are defined analogously. The first operator leads to a transition stress parameter $\mathcal{A}_1$ which is defined exactly as for centers of T_d symmetry. Matrix elements of the second operator vanish in DPA but will, for the deep ground states of chalcogen pairs, be responsible for the lifting of the orientational degeneracy. We define the transition stress parameter $\mathcal{A}_2$ as

$$\mathcal{A}_2=\frac{1}{2}\frac{1}{\sqrt{3}}(\langle e|V_{A_1'}|e\rangle-\langle g|V_{A_1'}|g\rangle) \ . \tag{13}$$

Our analysis shows that the excited states are well described by DPA and that the excited electron does not contribute to $\mathcal{A}_2$. For a single donor in a one-electron picture $\mathcal{A}_2$ will be determined by the ground state to the extent that it deviates from EMT. For a double donor, neither $\mathcal{A}_1$ nor $\mathcal{A}_2$ can simply be interpreted in terms of one-particle level shifts.

The labels $\mathcal{A}_1$ and $\mathcal{A}_2$ and their respective definitions are chosen to comply with Ref. 27, where the perturbation is defined as a function of stress and not of strain, which again introduces compliance tensor elements into our expressions for the shifts. Using the strain tensor for different stress directions, we obtain the shifts and splittings of the ground states of orientationally degenerate C_{3v} or D_{3d} centers given in Table IV. It is important to remember that the splitting of the ground state is due to the crystallographic inequivalence of different centers, thus no thermalization effects occur as long as the ground states are well below the Fermi level. In addition to the effects associated with the ground state of orientationally degenerate centers, we have to consider the effects of stress on the electronic degeneracy of the excited states.

TABLE IV. Stress dependence of the ground states of orientationally degenerate centers with C_{3v} or D_{3d} symmetry.

Stress direction	Relative intensity	Shift in energy
[001]	4	$\mathcal{A}_1(s_{11}+2s_{12})T$
[110]	2	$\left[\mathcal{A}_1(s_{11}+2s_{12})+\frac{\mathcal{A}_2 s_{44}}{2}\right]T$
	2	$\left[\mathcal{A}_1(s_{11}+2s_{12})-\frac{\mathcal{A}_2 s_{44}}{2}\right]T$
[111]	1	$\left[\mathcal{A}_1(s_{11}+2s_{12})+\mathcal{A}_2 s_{44}\right]T$
	3	$\left[\mathcal{A}_1(s_{11}+2s_{12})-\frac{\mathcal{A}_2 s_{44}}{3}\right]T$

As an example we expect the $1s(A_1)\rightarrow 2p_\pm$ absorption line in C_{3v} or D_{3d} symmetry to split into four lines for a stress along the [110] axis.

IV. RESULTS

A. D^0 centers

Figures 3 and 4 show the splitting of the higher excited states of S^0 and Se^0. The splitting patterns and polarization selection rules are entirely consistent with the expected behavior of T_d donors described by EMT and DPA. In all the measurements, the $1s(A_1)\rightarrow 2p_\pm$ transition energies for the three stress directions were fitted to our parametrized linear theory using multiple regression analysis, weighing each direction by the corresponding inverse variance in slope. We obtain $\Xi_u = 8.7\pm0.5$ eV $[(7.0\pm0.4)\times10^4$ cm$^{-1}]$ for the shear deformation potential constant of S^0 and $\Xi_u = 8.5\pm0.4$ eV $[(6.8\pm0.4)\times10^4$ cm$^{-1}]$ for Se^0. The errors were estimated by adding the errors of the slopes, the pressure, and the sample area. All other relative errors were at least an order of magnitude smaller. The area turns out to be the most critical parameter, and since our samples were small compared to, for example, those of Tekippe *et al.*,[24] the relative error becomes quite large: we estimate it to be 3%; the error in pressure is estimated to 2%. For all calculations where values of the compliance tensor components were needed, we use the 4.2-K values of Hall:[28] $s_{11}-s_{12} = 9.745\times10^{-12}$ m^2/N, $s_{11}+2s_{12} = 3.363\times10^{-12}$ m^2/N, and $s_{44} = 1.246\times10^{-11}$ m^2/N. These values should not change significantly between 4.2 K and our measurement temperatures of around 10 K. The ground-state stress parameters obtained are $\mathcal{A}_1 = 1.0\pm0.06$ eV $[(8.0\pm0.5)\times10^3$ cm$^{-1}]$ for S^0 and $\mathcal{A}_1 = 0.89\pm0.07$ eV $[(7.1\pm0.6)\times10^3$ cm$^{-1}]$ for Se^0.

Figures 5 and 6 show the splitting of the $1s(A_1)\rightarrow 1s(T_2)$ transitions of the S^0 and Se^0 centers. The $1s(T_2)$ state has the same symmetry as the np_0 states and thus the polarization selection rules are the same. For [110] stress, the upper branch shows a complicated behavior, which we attribute to an avoided crossing of a component of the $1s(T_2)$ state with a component of the $1s(E)$ state to which dipole transitions are symmetry forbidden at zero stress.[7] Figures 7(a) and 7(b) show qualitatively how the $1s(T_2)$ and $1s(E)$ states are expected to split under uniaxial stress for stresses along [001] and [110]. For stress along [001] the point group is reduced from T_d to D_{2d},and for [110] stress to C_{2v}. The components of the states are labeled with the irreducible representations of the respective point group according to which they transform. Equal-symmetry components may interact, whereby the crossing components are mixed and both become visible in absorption. When components of different symmetry cross, no coupling is expected, and in fact no effect is seen at the other crossings in Fig. 7. From the expected linear behavior of the $1s(E)$ components we can estimate the $1s(E)$ binding energy to be 31.7 meV for S^0 and 31.4 meV for Se^0. These values agree well with those obtained from the study of phonon-assisted Fano resonances,[10] and thus confirm the previous assignment.

In the lower branches of the Se^0 spectra, another avoided crossing is observed. As shown in a previous paper,[8] the interacting state in this case is a component of a level from the spin-triplet $1s(T_2)$ term and the interaction which mixes the two components is the spin-orbit (s.o.) interaction. Due to the smaller s.o. interaction of the lighter element sulfur, no crossing and thus no coupling is observed in the S^0 spectra. For the heavier chalcogen tellurium,[8] the effect becomes much more pronounced due to the larger s.o. interaction. Tuning the energy level separation of the spin-singlet and spin-triplet terms by uniaxial stress, one effectively tunes the interaction between these levels, so that also spin-triplet states become visible in optical absorption at near-resonance when their mixing with spin-singlet states due to the s.o. interaction becomes sufficiently strong.

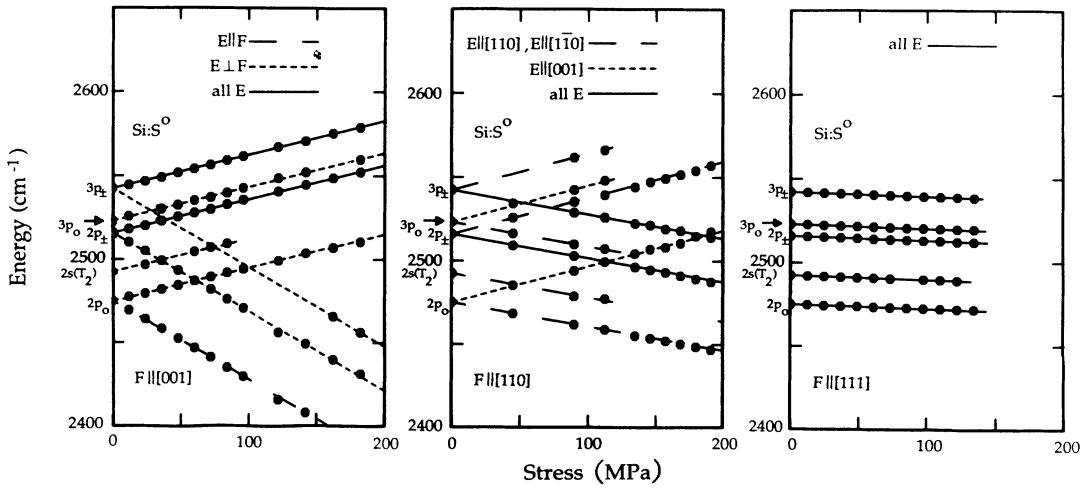

FIG. 3. Stress dependence of transitions from the ground state to the higher excited states of S^0. The lines are drawn using parameters obtained from a fit to the $1s(A_1)\rightarrow 2p_\pm$ transitions.

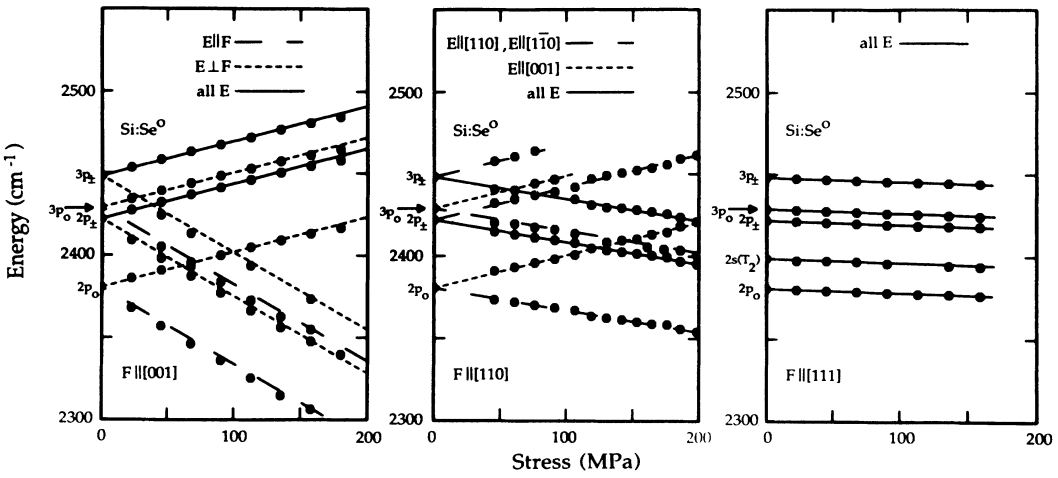

FIG. 4. Stress dependence of transitions from the ground state to the higher excited states of Se^0. The lines are drawn using parameters obtained from a fit to the $1s(A_1) \rightarrow 2p_\pm$ transitions.

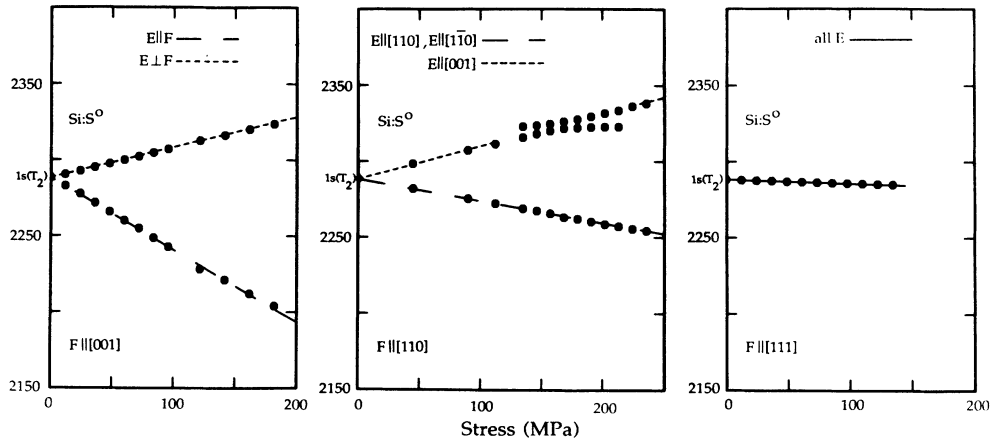

FIG. 5. Stress dependence of transitions from the ground state to the $1s(T_2)$ state of S^0. The lines are drawn using parameters obtained from a fit to the $1s(A_1) \rightarrow 2p_\pm$ transitions. The complicated behavior observed in the upper branch of the **F**||[110] spectrum is due to an avoided crossing with a component of the $1s(E)$ state, to which dipole transitions are forbidden. At near-resonance the states are mixed, and both transitions are observed over a limited stress range.

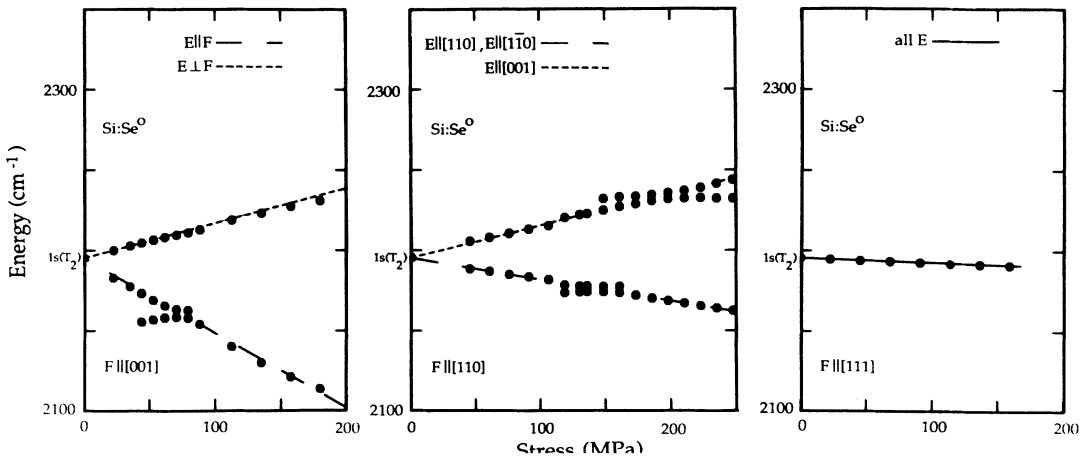

FIG. 6. Stress dependence of transitions from the ground state to the $1s(T_2)$ state of Se^0. The lines are drawn using parameters obtained from a fit to the $1s(A_1) \rightarrow 2p_\pm$ transitions. The behavior observed in the upper branch of the **F**||[110] spectrum is due to an avoided crossing with a component of the $1s(E)$ state, to which dipole transitions are forbidden. At near-resonance the states are mixed, and both transitions are observed over a limited stress range. In the lower branch of the **F**||[001] and **F**||[110] spectra, avoided crossings with a component from the dipole-forbidden spin-triplet $1s(T_2)$ level are observed.

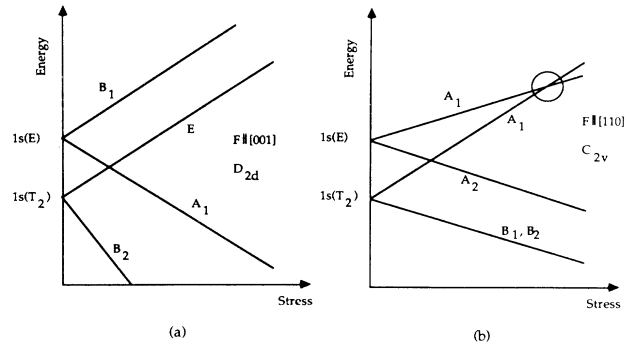

FIG. 7. Schematic splitting diagram of the $1s(T_2)$ and $1s(E)$ states for (a) [001] and (b) [110] stress. The components of the stress-split states are labeled by the irreducible representations of the appropriate point group. Crossing components of the same symmetry may interact, as indicated by the circle in the upper branch of the $1s(T_2)$ state for stress along [110].

B. D^+ centers

Uniaxial-stress spectra of the higher excited states of S^+ and Se^+ are given in Figs. 8 and 9. The charge of the center is manifest as a fourfold increase in the binding energies of the excited states. In our sulfur doped samples, electric field broadening effects[3] due to charged acceptors in the originally p-type material made the $1s(A_1)\rightarrow 3p_\pm$ line very broad, which made accurate measurements of this line difficult. The spectral line of S^+ assigned by Krag *et al.*[11] to be a $2p_0$ replica we interpret as the $2s(T_2)$ state, or $2s(\Gamma_7+\Gamma_8)$ if spin is included. The line is too broad for the spin-orbit splitting between Γ_7 and Γ_8 to be resolved (see below). At first glance, the spectra seem to follow DPA for a T_d center rigorously, and the splitting of the respective $2p_\pm$ lines give the following values for the deformation potential constants and ground-state stress parameters: $\Xi_u=8.2\pm0.4$ eV $[(6.7\pm0.4)\times10^4$ cm$^{-1}]$ and $\mathcal{A}_1=1.2\pm0.08$ eV $[(9.5\pm0.7)\times10^3$ cm$^{-1}]$ for S^+, $\Xi_u=8.2\pm0.4$ eV $[(6.6\pm0.4)\times10^4$ cm$^{-1}]$ and $\mathcal{A}_1=1.4\pm0.1$ eV $[(12\pm0.8)\times10^3$ cm$^{-1}]$ for Se^+. Studying the splitting of the $2p_0$ and $2s(\Gamma_7+\Gamma_8)$ states of Se^+ for stress along [110], however, one finds two lines in the upward-going component (Fig. 9) where only one line is expected. For the $2s(\Gamma_7+\Gamma_8)$ component two lines are observed in a limited stress range only, which may indicate that some kind of avoided crossing takes place. In the case of $2p_0$, both lines are clearly visible up to the highest stresses once they appear. If these anomalous splittings were due to inhomogeneous or misaligned stress, one would expect to see similar effects for all lines, including the $2p_\pm$ and $3p_0$ lines, which is not the case. We have at present no explanation for the extra splitting observed.

The $1s(T_2)$ state of S^+ and Se^+ have binding energies of 184 meV (1480 cm^{-1}) and 164 meV (1320 cm^{-1}), consequently they are the deepest excited states of the chalcogen donor set. The spin-orbit interaction is proportional to the gradient of the electronic potential; an electron in these states is highly localized near the impurity, and thus it will be strongly affected by this interaction. The $1s(T_2)$ is found to split into a $1s(\Gamma_7)$ (corresponding to $J=\frac{1}{2}$) and a $1s(\Gamma_8)$ state (corresponding to $J=\frac{3}{2}$); the binding energies given above are weighted means of the $1s(\Gamma_7)$ and $1s(\Gamma_8)$ energies.

The s.o. interaction can be combined with the stress

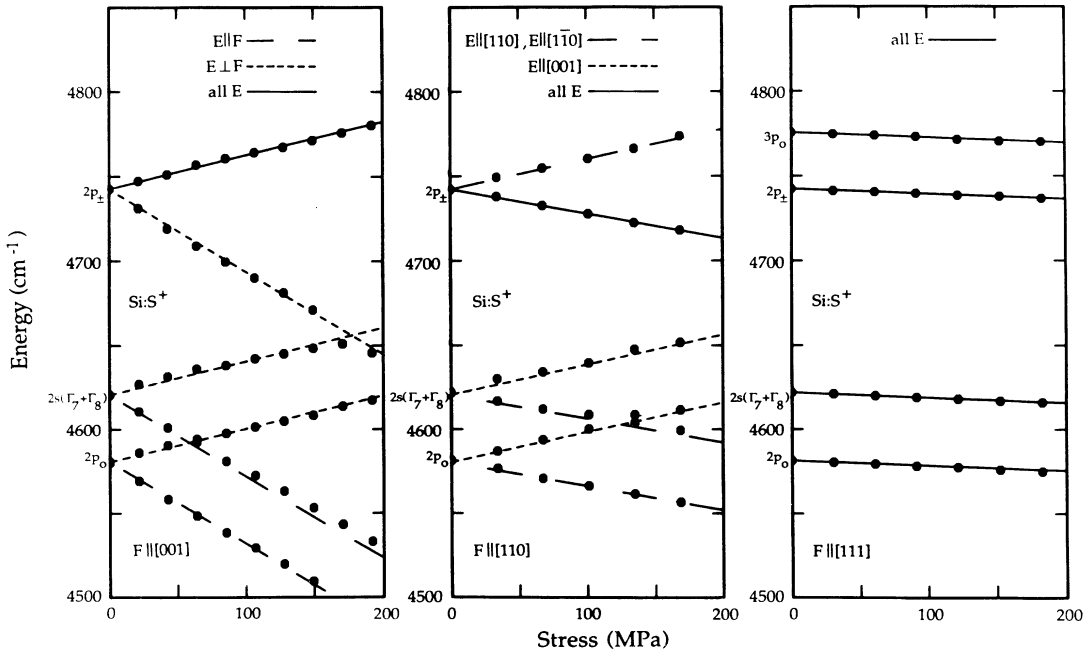

FIG. 8. Stress dependence of transitions from the ground state to the higher excited state of S^+. The lines are drawn using parameters obtained from a fit to the $1s(A_1)\rightarrow 2p_\pm$ transitions.

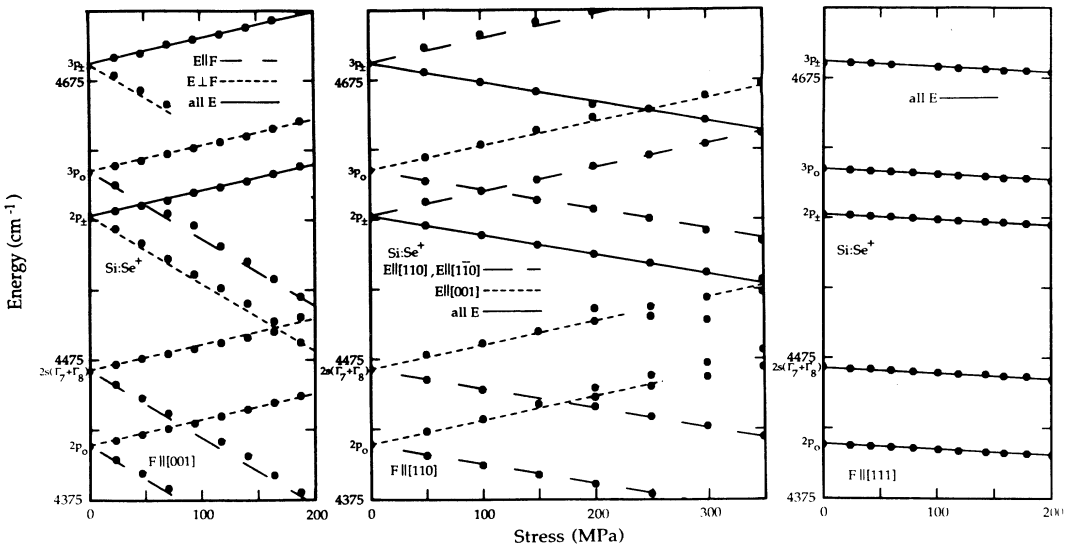

FIG. 9. Stress dependence of transitions from the ground state to the higher excited states of Se^+. The lines are drawn using parameters obtained from a fit to the $1s(A_1)\rightarrow 2p_{\pm}$ transitions. For F||[110] a strange behavior of the upper components of the transition lines $1s(A_1)\rightarrow 2p_0$ and $1s(A_1)\rightarrow 2s(\Gamma_7+\Gamma_8)$ is observed. In the case of the $2s$ transition, an avoided crossing seems to take place, similar to the $1s(T_2)-1s(E)$ crossings observed for the S^0 and Se^0 centers.

dependence from DPA.[9] However, it turns out that such an s.o. extended DPA is not able to describe the stress dependence of the $1s(T_2)$ states of S^+ and Se^+, and therefore the more general approach described in Sec. III C has to be used. The stress dependence of the $1s(A_1)\rightarrow 1s(\Gamma_7)$ and $1s(A_1)\rightarrow 1s(\Gamma_8)$ transitions of S^+ and Se^+ are shown in Figs. 10 and 11. The behavior predicted by the DPA together with a linear ground-state shift is indicated by dashed lines. As can be seen, the splitting for both centers is smaller than expected: by a factor of 0.37 for S^+ and by 0.55 for Se^+, reflecting the deviation of the parameter $\mathcal{B}'$ defined in Eq. (11) from its DPA value $\Xi_u/3$.

The darker lines drawn in Figs. 10 and 11 have been obtained from a numerical fit to the data. The parameters in the fit included the reduction factor of the splitting, as well as linear and quadratic shifts of the center of gravity of the lines. The quadratic term was included *ad hoc* since it obviously improved the fit, but it has no foundation in our linear theory. Since the deeper ground state shifts linearly, we expect this nonlinearity rather to be due to an interaction between states than to quadratic stress effects. For S^+, we clearly observe a splitting of the upper components for F||[111], and also an unexpected divergence of the two lower components for F||[110]. These two effects are easily accounted for by including

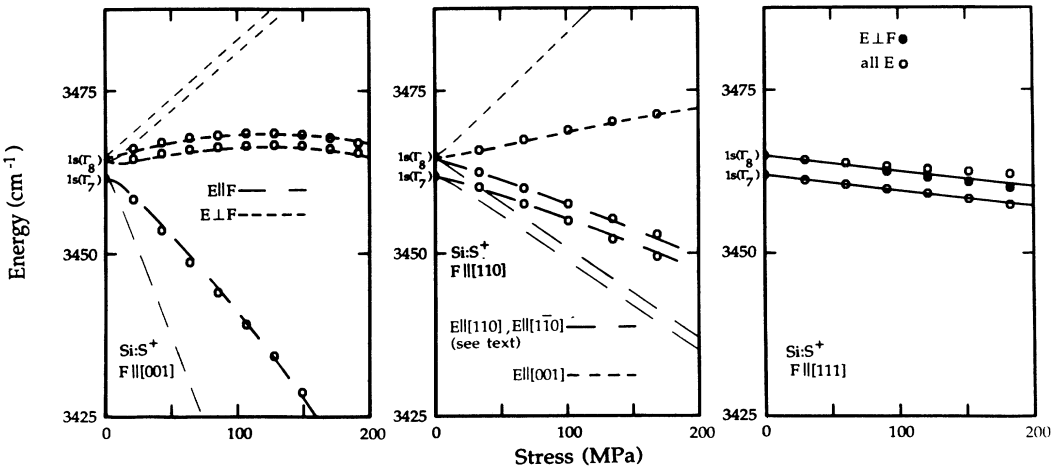

FIG. 10. Stress dependence of transitions from the ground state to the $1s(\Gamma_7)$ and $1s(\Gamma_8)$ state of S^+. The darker lines are obtained from a numerical fit discussed in the text. The lighter lines indicate the stress dependence expected from the deformation-potential approximation (DPA).

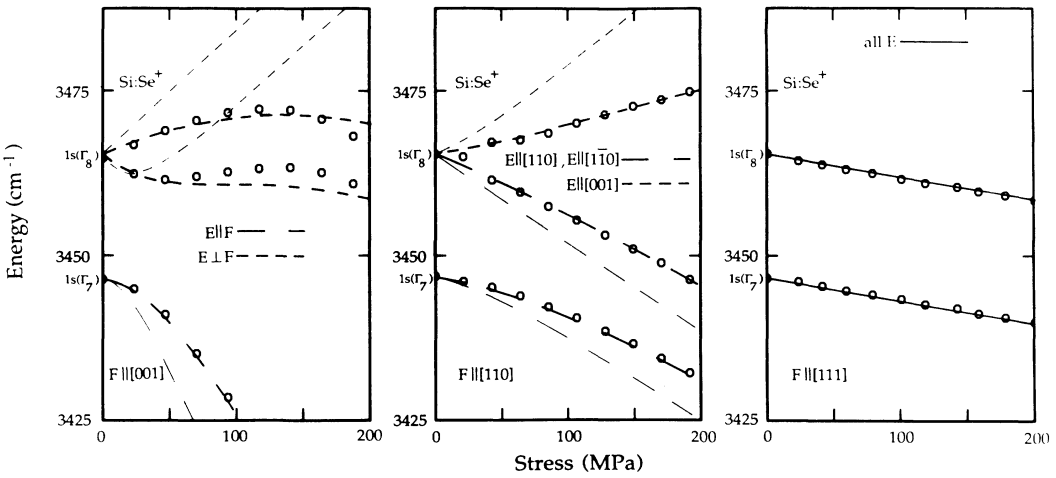

FIG. 11. Stress dependence of transitions from the ground state to the $1s(\Gamma_7)$ and $1s(\Gamma_8)$ state of Se^+. The darker lines are obtained from a numerical fit discussed in the text. The lighter lines indicate the stress dependence expected from the deformation-potential approximation (DPA).

stress perturbation operators of T_2 symmetry, i.e., including the parameter $\mathcal{C}$ defined in Eq. (12), for which we obtain a value of $\mathcal{C}=-0.15$ eV (-1.2×10^3 cm^{-1}). The effect from a similar value of $\mathcal{C}$ for Se^+ would be much smaller due to the larger spin-orbit splitting. Since no effect was observed experimentally for this center, no value of $\mathcal{C}$ for Se^+ could be determined.

The most prominent effect of the T_2 operators for [110] stress lies in the polarization selection rules. From DPA, we would expect to see both the lower components for **E**||[110] and **E**||[1$\bar{1}$0], which indeed is observed for Se^+. For S^+ at higher stresses, the lowest component is only visible for **E**||[1$\bar{1}$0], whereas the second lowest is visible only for **E**||[110]. The observed variations of transition probabilities are entirely consistent with the obtained value of $\mathcal{C}$.

C. $D_2{}^0$ centers

These centers consist of pairs of impurity atoms oriented along the ⟨111⟩ axes of the crystal. The trigonal symmetry has virtually no effect on the *np* states, which follow EMT within experimental accuracy. The stress dependence of the transitions from the $1s(A_1^+)$ ground state to the higher excited states of $S_2{}^0$ and $Se_2{}^0$ are shown in Figs. 12 and 13. The splitting patterns are in agreement with the discussion above; the *np* states are described by DPA and the ground states of inequivalent centers shift as described in Table III. The polarization selection rules fully corroborate this interpretation. Numerical fits to the $2p_\pm$ splitting of the two centers give $\Xi_u=8.8\pm0.5$ eV [$(7.1\pm0.4)\times10^4$ cm^{-1}], $\mathcal{A}_1=0.44\pm0.05$ eV [$(3.6\pm0.4)\times10^3$ cm^{-1}], and $\mathcal{A}_2=-1.5\pm0.08$ eV

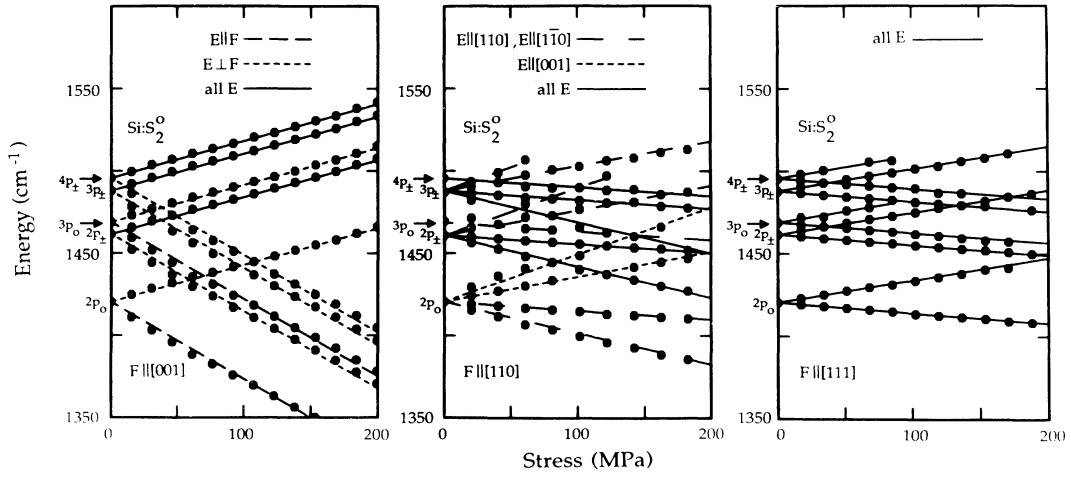

FIG. 12. Stress dependence of transitions from the ground state to the higher excited state of $S_2{}^0$. The lines are drawn using parameters obtained from a fit to the $1s(A_1)\rightarrow 2p_\pm$ transitions.

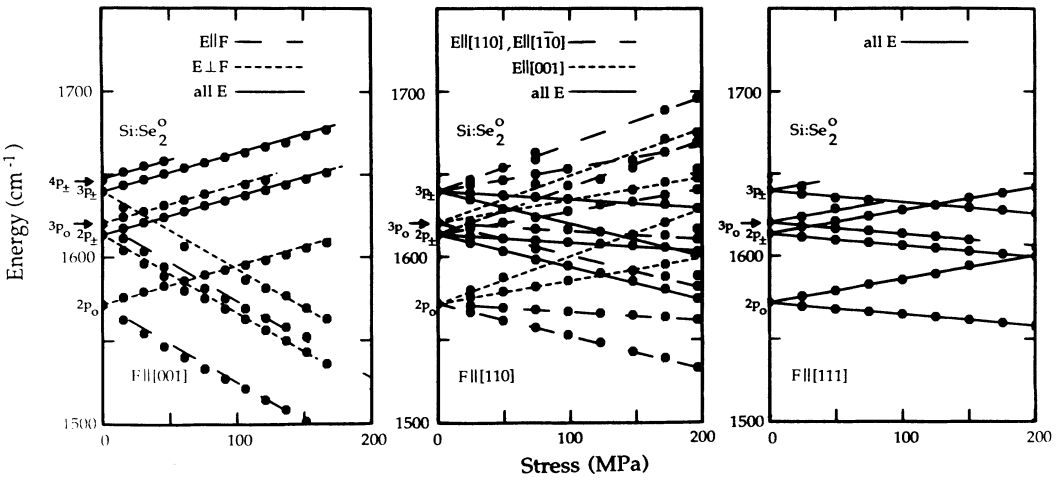

FIG. 13. Stress dependence of transitions from the ground state to the higher excited state of Se_2^0. The lines are drawn using parameters obtained from a fit to the $1s(A_1)\rightarrow 2p_\pm$ transitions.

$[(-1.2\pm0.06)\times10^4\ \text{cm}^{-1}]$ for S_2^0, and $\Xi_u=8.5\pm0.5$ eV $[(6.9\pm0.4)\times10^4\ \text{cm}^{-1}]$, $\mathcal{A}_1=0.55\pm0.06$ eV $[(4.5\pm0.5)\times10^3\ \text{cm}^{-1}]$, and $\mathcal{A}_2=-1.5\pm0.08$ eV $[(-1.2\pm0.07)\times10^3\ \text{cm}^{-1}]$ for Se_2^0.

As mentioned above, the $1s$ state is split into $1s(A_1^+)$, $1s(E^+)$, $1s(A_1^-)$, and $1s(E^-)$ by the valley-orbit interaction. Parity selection rules forbid transitions between equal parity states, and thus only two absorption lines are observed at zero stress due to $1s(A_1^+)\rightarrow 1s$ transitions. The stress dependence of these transitions are shown in Figs. 14 and 15, and from the splitting pattern it is quite obvious that the state with the greater binding energy of the two is the $1s(E^-)$ state, which lies close to the EMT value of 31.26 meV. The $1s(A_1^-)$ state actually has a lower binding energy than predicted by EMT. A possible explanation of this effect is offered by the calculations of Sankey and Dow.[20] They find that two of the pair's four extra valence electrons are in an A_1^- state near the valence band. Orthogonalization effects may lead to repulsion between this A_1^- state and the $1s(A_1^+)1s(A_1^-)$ configuration of the double donor.

From Figs. 14 and 15 we see that the splitting of the $1s(A_1^+)\rightarrow 1s$ transitions is nonlinear, in contrast to the $1s(A_1^+)\rightarrow np$ transitions. This is an effect of the mixing of the a_1 and θ states discussed in Sec. III B. The lines in Figs. 14 and 15 have been drawn taking into account this mixing of the a_1 and θ states as given by the DPA, using stress parameter values obtained by fitting the $1s(A_1^+)\rightarrow 2p_\pm$ splitting. Obviously, a more general treatment as used in Ref. 11 is not required. The theoretical polarization selection rules for $A_1\rightarrow A_1$ transitions under uniaxial stress have been given by Kaplyanskii[27] and for $A_1\rightarrow E$ transitions by Hughes and Runciman.[29] We find that our results are in good agreement with these predictions. In some cases, however, we were unable to detect lines which are predicted to have a small but finite strength. This was probably due to our limited signal-to-noise ratio.

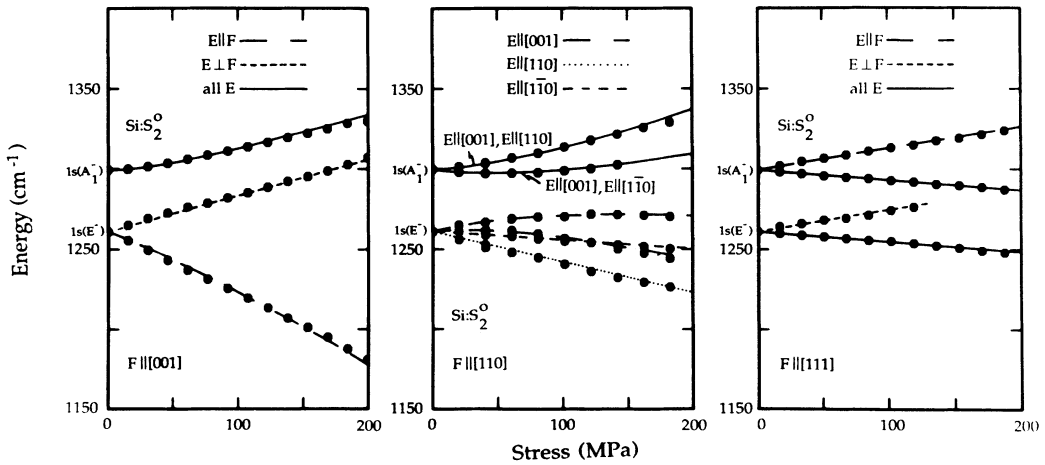

FIG. 14. Stress dependence of transitions from the ground state to the $1s(E^-)$ and $1s(A_1^-)$ states of S_2^0. The lines are drawn using parameters obtained from a fit to the $1s(A_1)\rightarrow 2p_\pm$ transitions. The nonlinear stress dependence for F||[001] and F||[110] clearly indicates a coupling of components of the two states.

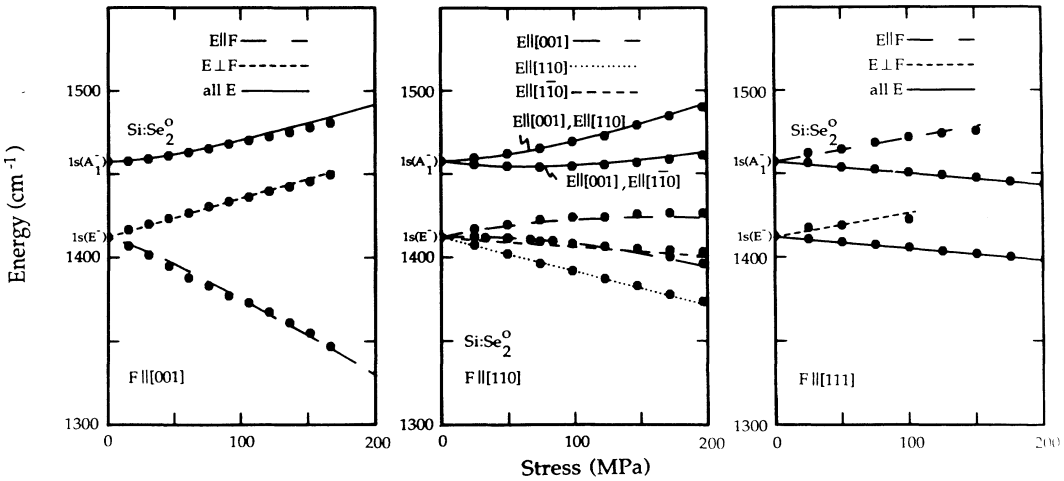

FIG. 15. Stress dependence of transitions from the ground state to the $1s(E^-)$ and $1s(A_1^-)$ states of Se_2^0. The lines are drawn using parameters obtained from a fit to the $1s(A_1)\rightarrow 2p_\pm$ transitions. The nonlinear stress dependence for **F**||[001] and **F**||[110] clearly indicates a coupling of components of the two states.

D. D_2^+ centers

Since we were not able to produce enough Se_2^+ centers in any of our samples for reliable measurements, only the S_2^+ center was studied. The S_2^+ center has a binding energy of 371.1 meV. For this center, the trigonal symmetry produces comparatively large effects, in that also p states are observed to split into an A_1^- and an E^- state at zero stress: the $2p_\pm$ is split by 0.3 meV and the $2p_0$ by 1.4 meV.[2] The $2p_0$ states appear substantially broadened; Janzén *et al.*[2] attempted to explain this by lifetime effects due to resonant phonon interaction, similar to the case of Si:Bi.[18] In contrast to Si:Bi, however, the broadening remains when the lines are shifted by stress. Thus some other mechanism has to be involved in the observed broadening.

The stress dependence of the higher excited states is shown in Fig. 16. Due to electric field broadening in our samples, transitions to $3p_\pm$ and higher states were not observed. Since the $2p_\pm$ line is split already at zero stress, it

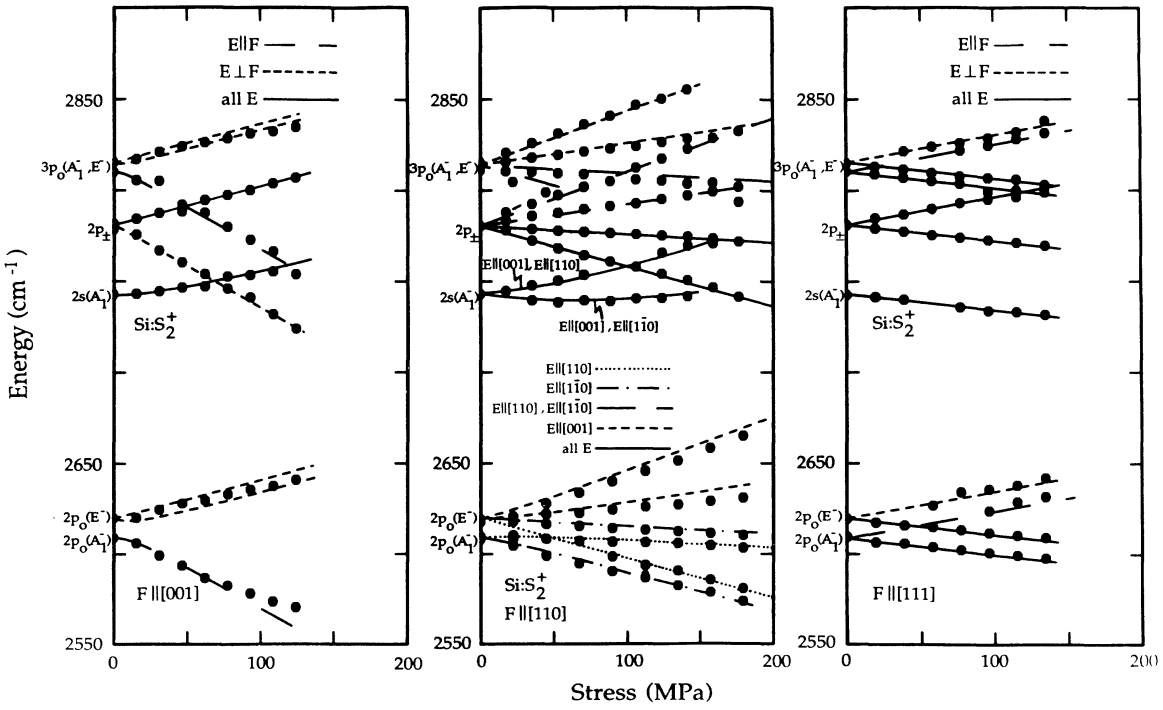

FIG. 16. Stress dependence of transitions from the ground state to the higher excited state of S_2^+. The lines are drawn using parameters obtained from a fit to the $1s(A_1)\rightarrow 2p_\pm$ transitions. The coupling of $2p_0(A_1^-)$ and $2p_0(E^-)$ and of $2s(E^-)$ and $2s(A_1^-)$ leads to nonlinear behavior of lines for **F**||[001] and **F**||[110].

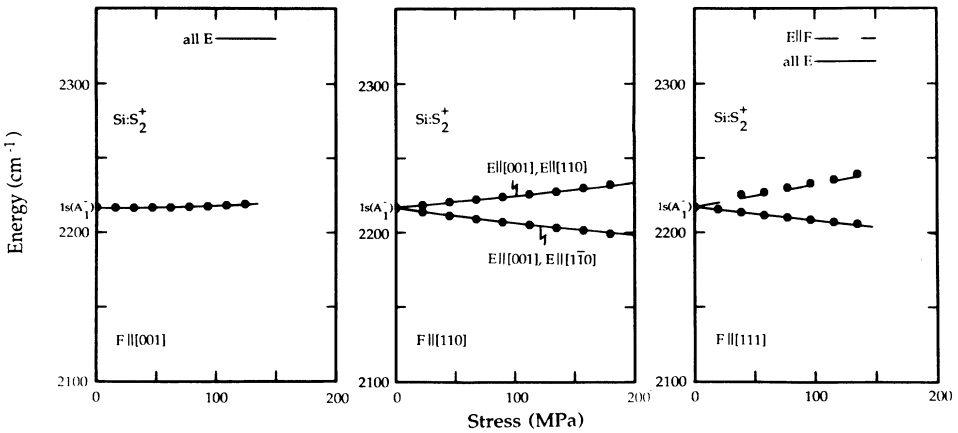

FIG. 17. Stress dependence of transitions from the ground state to the $1s(A_1^-)$ state of S_2^+. The lines are drawn using parameters obtained from a fit to the $1s(A_1)\rightarrow 2p_\pm$ transitions. The nonlinear stress dependence for F||[001] and F||[110] clearly indicates a coupling of components of the $1s(A_1^-)$ and $1s(E^-)$.

is difficult to make a reliable fit. Furthermore, a small inhomogeneity in the stress makes the two lines at zero stress merge into one as the stress is increased. In spite of this, the $2p_\pm$ components were still the best lines for the numerical fit, from which we obtained $\Xi_u = 8.5\pm0.4$ eV [$(6.8\pm0.4)\times10^4$ cm^{-1}], $\mathcal{A}_1 = 0.81\pm0.11$ eV [$(6.5\pm0.9)\times10^3$ cm^{-1}], and $\mathcal{A}_2 = -1.8\pm0.1$ eV [$(-1.4\pm0.08)\times10^4$ cm^{-1}] for this center. Using these parameters and accounting for the mixing of the a_1 and θ states within DPA (Sec. II B), we obtain the lines drawn for the $2p_0$ components. The fit is good, especially if one considers the width of the lines, which also made it impossible to resolve the two lines going towards higher energies for [001] stresses.

The $1s(A_1^+)\rightarrow 2s(A_1^-)$ transition shows a stress dependence which indicates interaction with the $2s(E^-)$ state. We did not observe any absorption line which could be assigned to this state, but from a simple fit of the $1s(A_1^+)\rightarrow 2s(A_1^-)$ stress dependence and assuming DPA matrix elements we obtained an estimated $1s(A_1^+)\rightarrow 2s(E^-)$ zero stress transition energy of 2709 cm^{-1}. This value was used when drawing the figure for the $1s(A_1^+)\rightarrow 2s(A_1^-)$ transition.

In Fig. 17 we present the splitting of the $1s(A_1^+)\rightarrow 1s(A_1^-)$ transition. The splitting pattern shows some effect from coupling to the $1s(E^-)$ state, and the polarization selection rules are entirely consistent with those given by Kaplyanskii.[27] The $1s(E^-)$ state almost exactly coincides with the $2p_\pm$ state of a sulfur-related complex, designated $S_c^+(X_1)$ by Janzén *et al.*[2] In our samples the concentration of this complex was too high to enable us to perform any measurements on the $1s(E^-)$ state of S_2^+.

V. DISCUSSION

From our experiments we conclude that the *np* states of all the chalcogen donors studied under uniaxial stress behave according to the DPA. Since the binding energies of these states are accurately given by EMT, the validity of EMT apparently implies the applicability of DPA. Hence, one can, e.g., determine the shear deformation potential Ξ_u from the splitting of the *np* states. Averaging over the values of Ξ_u for the different centers given in Table V we obtain $\Xi_u = 8.5\pm0.2$ eV [$(6.8\pm0.2)\times10^4$ cm^{-1}]. This value compares well with the value $\Xi_u = 8.77\pm0.07$ eV obtained from measurements on shallow donors by Tekippe *et al.*[24] Krag *et al.*[11] have previously quoted a value of $\Xi_u = 7.9$ eV (no error bars given) for sulphur centers. Li *et al.*[30] obtained a value of $\Xi_u = 11$ eV for chalcogen centers in Si from DLTS (deep level transient spectroscopy).

The stress dependence of the $1s(A_1)\rightarrow 1s(T_2)$ transitions at D^0 and the corresponding transitions at D_2 centers are found to be well described by the DPA, although the ionization energies of the $1s(T_2)$ states may

TABLE V. Stress parameters obtained from experiment in the present study.

Center	Ξ_u (eV) [Ξ_u (cm^{-1})]	$\mathcal{A}_1$ (eV) [$\mathcal{A}_1$ (cm^{-1})]	$\mathcal{A}_2$ (eV) [$\mathcal{A}_2$ (cm^{-1})]
S_2^0	8.8 ± 0.5 [$(7.1\pm0.4)\times10^4$]	0.44 ± 0.05 [$(3.6\pm0.4)\times10^3$]	-1.5 ± 0.08 [$(-1.2\pm0.06)\times10^4$]
Se_2^0	8.5 ± 0.5 [$(6.9\pm0.4)\times10^4$]	0.55 ± 0.06 [$(4.5\pm0.5)\times10^3$]	-1.5 ± 0.08 [$(-1.2\pm0.07)\times10^4$]
Se^0	8.5 ± 0.4 [$(6.8\pm0.4)\times10^4$]	0.89 ± 0.07 [$(7.1\pm0.6)\times10^3$]	
S^0	8.7 ± 0.5 [$(7.0\pm0.4)\times10^4$]	1.0 ± 0.06 [$(8.0\pm0.5)\times10^3$]	
S_2^+	8.5 ± 0.4 [$(6.8\pm0.4)\times10^4$]	0.81 ± 0.11 [$(6.5\pm0.9)\times10^3$]	-1.8 ± 0.1 [$(-1.4\pm0.08)\times10^4$]
Se^+	8.2 ± 0.4 [$(6.6\pm0.4)\times10^4$]	1.4 ± 0.1 [$(12\pm0.8)\times10^3$]	
S^+	8.2 ± 0.4 [$(6.7\pm0.4)\times10^4$]	1.2 ± 0.08 [$(9.5\pm0.7)\times10^3$]	

differ by a few meV from the EMT value. It should be noted that for the impurity pairs, it is necessary to take into account the matrix elements introduced by DPA which couple the $ns(A_1^-)$ and $ns(E^-)$ states. For all these nearly EMT-like excited states the wave function seems to be sufficiently localized at the conduction-band minima for DPA to be valid. Thus the behavior under stress is well understood and one can in detail analyze the observed avoided crossings between optically forbidden and allowed final states. From such studies the zero-stress binding energy of the $1s(E)$ state of D^0 could be inferred, confirming the previous prediction based on phonon-assisted Fano resonances, and spin-triplet $1s(T_2)$ states, or strictly speaking, spin-triplet terms of the $1s(A_1)1s(T_2)$ configuration could be clearly identified. The applicability of DPA thus yields the possibility to shift final states in a controlled manner and thereby detect optically forbidden final states.

In contrast to the shallow excited states, the deep ground states of the chalcogen donors are not well described by EMT, and their stress dependence is not given by DPA. This is reflected in a shift of the centers of gravity of the $1s(A_1)\rightarrow np$ transitions when stress is applied. This shift is measured by the stress parameter $\mathcal{A}_1$, plotted in Fig. 18 versus ionization energy of the center. Within a one-particle picture, $\mathcal{A}_1$ thus determines the difference in stress dependence between the ground state and the conduction bands for the double donors in their singly ionized charge state. $\mathcal{A}_1$ tends to increase with increasing ground-state ionization energy. For the neutral double donors the initial state has two electrons in a $1s(A_1)$ orbital, in the final state the $1s(A_1)$ orbital is singly occupied. Assuming these orbitals in a first approximation to be the same, and further assuming the electron-electron interaction to be unaffected by the shift under stress of the initial-state $1s(A_1)$ orbital, $\mathcal{A}_1$ again measures the shift of this orbital relative to the conduction bands. $\mathcal{A}_1$ would in this case have the same value for the neutral and the ionized charge states of a given center. This is not found experimentally which can be explained by a non-negligible relaxation of the inner orbital upon excitation of the donor, which leads to different shift rates of the two orbitals. Also for the neutral donors one notes a trend of increasing $\mathcal{A}_1$ with increasing ionization energy, which reflects an increasing deviation of the $1s(A_1)$ orbital from EMT.

Other groups have studied chalcogen donors using DLTS under pressure. Li *et al.*[30] have used uniaxial stress, and Jantsch *et al.*[31] hydrostatic pressure. The pressure coefficients of the ground states obtained from these measurements may be compared if the hydrostatic coefficients are multiplied by $\frac{1}{3}$, since hydrostatic pressure on a cube may be viewed as simultaneous uniaxial stress

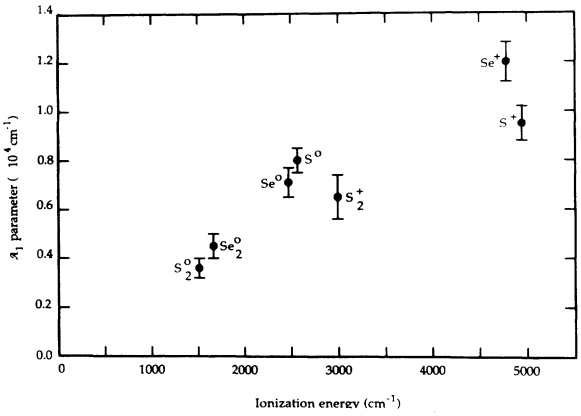

FIG. 18. Ground-state shift parameter $\mathcal{A}_1$ as a function of ionization energy.

from three perpendicular directions. With this normalization both groups obtain pressure coefficients corresponding to our parameter $\mathcal{A}_1$ that are approximately 1.5 times larger. It is unclear, however, whether ir and DLTS data may be compared directly. We feel that ir measurements are more direct and thus better suited for the purpose of obtaining pressure coefficients of electronic states.

The $1s(A_1)\rightarrow 1s(T_2)$ transitions at D^+ centers show considerable deviations from DPA also for the $1s(T_2)$ orbital of the excited electron. The greatly reduced splitting compared to DPA and the clear observation of an interaction between split components which is not predicted by DPA express the deep character of these excited states.

For the pairs D_2 a second stress parameter $\mathcal{A}_2$, which vanishes in DPA, expresses the lifting of the orientational degeneracy of these trigonal centers. Here the splitting pattern resulting from a nonzero $\mathcal{A}_2$ offers additional information on the symmetry of the center. For $\mathcal{A}_2$ we find values around -1.5 eV (cf. Table V). Krag *et al.*[11] define a parameter V, which is related to $\mathcal{A}_2$ through $\mathcal{A}_2=1.5V$. Even with this normalization the values of Krag *et al.* are slightly smaller than ours, consistent with their smaller value of Ξ_u.

In all cases where an approach beyond DPA was warranted, the data could be parameterized in terms of a perturbation taken to be linear in stress. The sole exceptions were the $1s(A_1)\rightarrow 1s(T_2)$ transitions at D^+ centers, where a quadratic shift of the center of gravity of the lines was introduced *ad hoc*, which, however, was attributed to a stress-induced interaction between states rather than a truly quadratic stress effect.

[1]P. Wagner, C. Holm, E. Sirtl, R. Oeder, and W. Zulehner, in *Festkörperprobleme: Advances in Solid State Physics*, edited by P. Grosse (Vieweg, Braunschweig, 1984), Vol. XXIV, p. 191.

[2]E. Janzén, R. Stedman, G. Grossmann, and H. G. Grimmeiss, Phys. Rev. B **29**, 1907 (1984).

[3]A. K. Ramdas and S. Rodriguez, Rep. Prog. Phys. **44**, 1297 (1981).

[4]G. W. Ludwig, Phys. Rev. **137**, A1520 (1965).

[5]J. R. Niklas and J.-M. Spaeth, Solid State Commun. **46**, 121

(1983).

[6]G. Grossmann, K. Bergman, and M. Kleverman, in *Proceedings of the Second International Conference on Shallow Impurity Centers, Trieste, 1986,* edited by A. Baldereschi and R. Resta (North-Holland, Amsterdam, 1987), p. 30.

[7]The neutral centers discussed in this paper are two-electron systems, thus we should be discussing transitions between configurations and not between states. However, since for all cases one electron remains in the ground state, no confusion should arise from the shorter notation chosen.

[8]K. Bergman, G. Grossmann, H. G. Grimmeiss, and M. Stavola, Phys. Rev. Lett. **56**, 2827 (1986); K. Bergman, G. Grossmann, H. G. Grimmeiss, M. Stavola, C. Holm, and P. Wagner, Phys. Rev. B **37**, 10 738 (1988).

[9]R. E. Peale, K. Muro, A. J. Sievers, and F. S. Ham, Phys. Rev. B **37**, 10 829 (1988).

[10]E. Janzén, G. Grossmann, R. Stedman, and H. G. Grimmeiss, Phys. Rev. B **31**, 8000 (1985).

[11]W. E. Krag, W. H. Kleiner, and H. J. Zeiger, Phys. Rev. B **33**, 8304 (1986).

[12]W. E. Krag, W. H. Kleiner, H. J. Zeiger, and S. Fischler, J. Phys. Soc. Jpn. Suppl. **21**, 230 (1966).

[13]W. Kohn, in *Solid State Physics,* edited by F. Seitz and D. Turnbull (Academic, New York, 1957), Vol. 5, p. 257.

[14]F. Beeler, M. Scheffler, O. Jepsen, and O. Gunnarsson, Phys. Rev. Lett. **54**, 2525 (1985).

[15]C. M. Weinert and M. Scheffler, Proceedings of the 14th International Conference on Defects in Semiconductors, Paris, 1986, edited by H. J. von Bardeleben [Mater. Sci. Forum **10-12**, 25 (1985); Phys. Rev. Lett. **58**, 1456 (1987).

[16]The Mulliken notation used is taken from M. Tinkham, *Group Theory and Quantum Mechanics* (McGraw-Hill, New York, 1964).

[17]M. Altarelli, in *Proceedings of the 16th International Conference on the Physics of Semiconductors, Montpellier, 1982,* edited by M. Averous (North-Holland, Amsterdam, 1983), p. 110.

[18]N. R. Butler, P. Fisher, and A. K. Ramdas, Phys. Rev. B **12**, 3200 (1975).

[19]W. E. Krag, W. H. Kleiner, and H. G. Zeiger, in *Proceedings of the 10th International Conference on the Physics of Semiconductors, Cambridge, Massachusetts, 1970,* edited by P. Keller, J. C. Hensel, and F. Stern (U.S.A.E.C., Division of Technical Information, Washington, D.C., 1970), p. 271.

[20]O. F. Sankey and J. D. Dow, Solid State Commun. **41**, 705 (1984).

[21]P. Wagner and C. Holm, in *Proceedings of the 13th International Conference on Defects in Semiconductors, Coronado, 1984,* edited by L. C. Kimerling, and J. M. Parsey, Jr. (Metallurgical Society of AIME, Warrendale, PA, 1985), p. 677.

[22]C. Herring, Bell Syst. Tech. J. **34**, 237 (1954).

[23]C. Herring and E. Vogt, Phys. Rev. **101**, 944 (1955).

[24]V. J. Tekippe, H. R. Chandrasekhar, P. Fisher, and A. K. Ramdas, Phys. Rev. B **6**, 2348 (1972).

[25]J. S. Griffith, *The Theory of Transition Metal Ions* (Cambridge University Press, London, 1961).

[26]A. A. Kaplyanskii, Opt. Spektrosk. **16**, 1031 (1964) [Opt. Spectrosc. (USSR) **16**, 557 (1964)].

[27]A. A. Kaplyanskii, Opt. Spektrosk. **16**, 602 (1964) [Opt. Spectrosc. (USSR) **16**, 329 (1964)].

[28]J. J. Hall, Phys. Rev. **161**, 756 (1967).

[29]A. E. Hughes and W. A. Runciman, Proc. Phys. Soc. London **90**, 827 (1967).

[30]M. Li, J. Chen, X. Zhao, and Y. Li, in Proceedings of the 14th International Conference on Defects in Semiconductors, Paris, 1986, edited by H. J. von Bardeleben [Mater. Sci. Forum **10-12**, 469 (1986)].

[31]W. Jantsch, K. Wünstel, O. Kumagai, and P. Vogl, in *Proceedings of the 16th International Conference on the Physics of Semiconductors, Montpellier, 1982,* edited by M. Averous (North-Holland, Amsterdam, 1983), p. 188.

[32]H. G. Grimmeiss, E. Janzén, and K. Larsson, Phys. Rev. B **25**, 2627 (1982).